Segment Density Distribution of Symmetric Diblock Copolymers at the Interface between Two Homopolymers As Revealed by Neutron Reflectivity

Thomas P. Russell,* Spiros H. Anastasiadis, and Alain Menelle

IBM Research Division, Almaden Research Center, 650 Harry Road, San Jose, California 95120-6099

Gian P. Felcher

Materials Science Division, Argonne National Laboratory, Argonne, Illinois 60439

S. K. Satija

Reactor Radiation Division, National Institute of Standards and Technology, Gaithersburg, Maryland 20899

Received September 18, 1990

ABSTRACT: The segment density distribution of symmetric, diblock copolymers of poly(styrene), PS, and poly(methyl methacrylate), PMMA, denoted P(S-*b*-MMA), were investigated by neutron reflectivity. Selective labeling of either block of the P(S-*b*-MMA) or of the PS or PMMA with deuterium provided the contrast necessary to isolate the distribution of the segments of the components at the interface. Results from a series of experiments were used to solve a simultaneous set of linear equations that yielded the segment density profiles of the PS and PMMA segments of the homopolymers and copolymers at the interface. It was found that the interface formed between the PS and PMMA segments could be described by a hyperbolic tangent function with an effective width of 75 Å. This width is 50% broader than that found between the PS and PMMA homopolymers in the absence of the diblock copolymer and between the PS and PMMA lamellar microdomains of the pure P(S-*b*-MMA) in the bulk. A significant penetration of the PS and PMMA homopolymers into the interfacial region was also found. The area occupied by the copolymer at the interface between the homopolymers is 30% larger than that of the copolymers in the bulk, lamellar microstructure.

1. Introduction

The mixing of two polymers is an attractive means by which the properties of polymers can be varied without the need of synthesizing new polymers. Unfortunately, most polymer pairs are immiscible and, consequently, coarsely phase separate upon mixing. In some cases, a dispersion of one polymer in another can be achieved by kinetically limiting the phase-separation process. However, even in those cases, due to the immiscibility, the interface between the phases is quite sharp and intermixing at the interface is minimal. This translates into a poor adhesion between the phases.

It is widely known that the presence of block or graft copolymers can alleviate, to some degree, the problems mentioned above. It is generally believed that this is a result of their ability to alter the interface between the homopolymer phases, acting as interfacial agents or compatibilizers for the immiscible polymers.[1-5] The interfacial activity of block copolymers has been shown to reduce significantly the interfacial tension between two immiscible homopolymers,[6] to permit a finer dispersion during mixing,[5,7] to provide stability against gross segregation upon thermal processing,[8] and to result in a dramatically improved interfacial adhesion.[9]

Theoretical attempts have been made to study the emulsifying effect of copolymers by Noolandi and co-workers,[10-12] Leibler,[13,14] and Duke.[15] Noolandi and Hong[10] used a general mean-field theory of inhomogeneous systems[16] based on the functional integral representation of the partition function[17] to model the behavior of the ternary system of two highly immiscible homopolymers, along with the corresponding diblock copolymer, diluted with a good solvent. They identified a number of factors that determine the state of the block copolymer in a phase-separated system. The entropy of mixing of the block copolymers with the homopolymers favors a random distribution of the copolymer chains. On the other hand, localization of the block copolymers at the interface displaces the homopolymers away from each other, thus lowering the enthalpy of mixing. In addition, each block of the copolymer will prefer to extend into the homopolymer with which it is miscible to lower the block copolymer–homopolymer enthalpy of mixing. In addition to the entropy loss due to the confinement of the copolymers to the interphase, there is a further entropy loss arising from the restriction of the blocks into their respective homopolymer regions. Finally, extension of the copolymer chains, as well as the effect of the excluded volume at the interphase for the homopolymers, leads to a further loss of entropy. Incorporating all these contributions into the free energy, Noolandi et al.[10-12] obtained the concentration of the block copolymer at the interface. A basic assumption of the theory was that the part of the copolymer that does not localize itself at the interface will be randomly distributed in the bulk of the homopolymers. However, micellar aggregation, rather than random distribution in the bulk of the homopolymers, could also occur. In this case, the micelles would compete with the interfacial region for the copolymer chains, and the amount of copolymers at the interface in micelles would depend on the relative reduction in the free energy as well as the surface area. Since the analysis of this more complicated case was not treated, their results can only be reliable for copolymer concentrations below the critical micelle concentration. Indeed, their predictions agree with interfacial tension

* To whom correspondence should be addressed.

0024-9297/91/2224-1575$02.50/0

data[6] for the initial reduction of the interfacial tension with diblock copolymer addition.

Leibler[13] investigated the nearly compatible mixture of two homopolymers A and B with the corresponding AB copolymer. For these systems, two mechanisms of the interfacial activity of the copolymer chains had to be distinguished: (i) there is more mixing of the A and B segments since copolymer chains are present in both phases, and (ii) the copolymer chains have a tendency to locate at the interface. For systems near the consolute point, where A and B are nearly miscible, the first mechanism dominates, whereas, for the highly incompatible case, the second is the dominant factor. Therefore, the mechanisms involved in the two different cases of highly immiscible systems compared to nearly compatible blends are quite different. In the first case, it is the surfactant activity of the block copolymer chains that causes the reduction in the interfacial tension. In the second case, the presence of copolymer molecules in the bulk homopolymer phases causes the compatibilizing behavior.

Leibler[14] investigated the case of highly incompatible systems, following the approach of de Gennes[18] to describe the interfacial activity of nonionic surfactants in oil–water mixtures. The copolymer joints are expected to localize in a thin interfacial layer with the blocks extending toward their respective bulk phases forming two "brushes". The approach is similar to the one successfully applied to the problem of polymer chains grafted to a surface.[19,20] Depending upon the molecular weight of the two homopolymers and the blocks of the copolymer and the interfacial area per copolymer joint, Σ, two different regimes were identified. For long copolymer chains and large Σ, the copolymers overlap strongly and stretch but the homopolymers can still penetrate the brushes (wet-brush case). For longer homopolymer chains and lower Σ, the copolymers are expected to be stretched and the homopolymer chains do not penetrate the copolymer layer appreciable (dry-brush case).

For both cases, the reduction in the interfacial tension induced by the copolymer adsorption under equilibrium conditions was calculated. The interfacial tension was found to decrease with the logarithm of the copolymer concentration up to the critical micelle concentration in the bulk phases. The possible existence of a thermodynamically controlled stable droplet phase was predicted in which the minority homopolymer particles, protected by an interfacial copolymer film, are suspended in a majority homopolymer matrix.

Duke[15] used a lattice Monte Carlo simulation based on a self-consistent mean-field approach to calculate the equilibrium interfacial properties of the three-component system: homopolymer A + homopolymer B + block copolymer AB. He calculated the interfacial profiles and the interfacial tension for different degrees of incompatibilities of the polymers and different concentrations, molecular weights, and structures of the copolymer. The copolymers chains were preferentially located in the interfacial region, and their excess amount increased rapidly with the bulk copolymer concentration. For copolymer concentrations less than a critical concentration, the segment density profiles of the A blocks in the A phase remained approximately Gaussian. The penetration depth of the copolymer segments into the respective phases was on the order of the radius of gyration of the copolymer. However, in the case of trapping higher concentrations of the copolymer, the AB joints are highly localized at the interface and the individual blocks are found to be stretched. In this case a significant interpenetration of homopolymer and copolymer chains occurs.

Table I
Homopolymer and Copolymer Characterization

	M_{PS}[a]	M_{PMMA}[a]	M_w/M_n	N_c[b]	f_{PS}[c]
P(S-*d*-*b*-MMA)	52 900	48 000	1.07	952	0.50
P(S-*b*-MMA-*d*)	56 300	65 000	1.12	1143	0.47
P(S-*d*-*b*-MMA-*d*)	55 900	59 200	1.10	1086	0.53
PS	127 000		1.05	1134	1.00
PS-*d*	110 000		1.05	982	1.00
PMMA		107 000	1.05	1070	0.00
PMMA-*d*		146 000	1.04	1352	0.00

[a] This represents the peak value of the molecular weight of the individual blocks. The results for the PS were obtained by extraction of a specimen after conclusion of the synthesis of the first block. The results for the PMMA were obtained from the difference between that of the copolymer and the PS block. [b] N_c is the total number of segments in the copolymer. [c] f_{PS} is the fraction of the copolymer, that is, PS.

Neutron reflectivity is sensitive to scattering length density gradients perpendicular to the surface of a film.[21] It has been successfully used to study polymer interfaces with excellent spatial resolution.[22-26] In this paper, neutron reflectivity has been used to investigate the segment density distribution of homopolymer and copolymer chains at the interface of a ternary system comprised of homopolymer A, homopolymer B, and diblock copolymer AB. Selective deuteration of either homopolymer chain or either block of the copolymer provides the contrast necessary to investigate the individual segment density distributions across the interface. It is shown that self-consistent density profiles can be determined by neutron reflectivity. Comparison of the measured profiles with current theories are presented.

2. Experimental Section

Poly(styrene-*b*-methyl methacrylate) symmetric, diblock copolymers where either the styrene or the methyl methacrylate block was perdeuterated were used in this study. The copolymers, purchased from Polymer Laboratories, Inc., were prepared by sequential anionic polymerization and were cleaned of residual polystyrene homopolymer by successive extractions in cyclohexane. The characteristics of the copolymers are given in Table I. The use of a letter "*d*" after the block denotes perdeuteration of that block. Polystyrene, PS, and poly(methyl methylacrylate), PMMA, homopolymers were also purchased from Polymer Laboratories, Inc., and were used as received. Their characteristics are also given in Table I. Specimens for the neutron reflectivity studies were prepared as follows. PMMA homopolymer is first spin-coated at 2000 rpm from toluene solution (~3.5 g/100 cm^3) onto a $\lambda/4$ optically polished Si disk (5.0 cm in diameter by 5 mm in thickness). The thickness of this layer was on the order of 2000 Å. This film was annealed for ca. 24 h above its glass transition temperature to remove any residual solvent and to allow the PMMA chains to relax. A thin diblock copolymer layer, with a thickness approximately equal to half of the long period of the neat ordered copolymer, i.e., ~200 Å, was spin-coated from toluene (~0.6 g/100 cm^3) onto a 7.5 cm × 12.5 cm glass microscope slide. The sides of the slide were scored with a razor blade, and the copolymer film was floated off onto a pool of deionized water. This was retrieved by using the substrate coated with the PMMA film. This bilayered specimen was allowed to air dry and then was placed onto a hot plate at 80 °C for 20 min. Next, a film of PS (~650 Å in thickness) was spin-coated onto a microscope slide, floated onto deionized water, and retrieved with the substrate coated with bilayer specimen. This trilayer specimen was allowed to dry in air and then was placed in a vacuum oven at 170 °C for a period of 5 or 10 days.

Initial experiments were designed to investigate bilayer specimens comprised of a layer of PS mixed with the copolymer on top of a layer of PMMA mixed with the copolymer. Such specimens were annealed for 240 h to allow the copolymer to migrate to the interface. However, reflectivity experiments

performed on specimens prepared in this manner exhibited a very large amount of diffuse off-specular scattering due, most likely, to the formation of micelles in the two phases. These bilayer specimens were, also, optically turbid after annealing, indicating the presence of large-size heterogeneities in the system. An approximate calculation of the critical micelle concentration (cmc) for this system gives values on the order of 10^{-6}–10^{-7} with the theories of Leibler[14] or Whitmore and Noolandi.[27] The trilayered configuration investigated here resembles more of a "trapping" of the copolymer molecules at the interface. However, as will be discussed later, after long annealing (120 h), the copolymer chains are found to extend deeply into the homopolymer domains, which is an indication of a large-scale movement of the polymeric chains. Experiments on the same specimens annealed for an additional 120 h showed no changes in the scattering length density profiles, indicating that at least the chains have attained a "local" equilibrium or a local minimum of the free energy.

Neutron reflectivity experiments were performed on POSY-II at the Intense Pulsed Neutron Source at Argonne National Laboratory. Details of the instrument can be found elsewhere.[28] In brief, a collimated (ca. 0.03°) beam of neutrons with a distribution of wavelengths, λ, between 2 and 16 Å impinged upon the surface of the specimen at a fixed angle, θ (typically $0.3° < \theta < 1.5°$). Specularly and off-specularly scattered neutrons are simultaneously detected with a linear position-sensitive gas detector. Due to the pulsed nature of the neutron source, the measurements are performed in a time-of-flight mode. The detection was done keeping the $\Delta\lambda/\lambda$ fixed. A "frame overlap" filter in front of the sample (a 100-mm Si disk with a layer of ^{58}Ni on top) at an angle of 1.4° eliminates neutrons with wavelengths larger than ca. 16 Å. This avoids errors associated with fast neutrons from one pulse being detected together with slow neutrons from the previous one. A ^{3}He pencil detector before the specimen is used to monitor the incident beam flux. This configuration allows the measurement of the reflectivity as a function of the component of the neutron momentum perpendicular to the film surface, $k_{0,z}$

$$k_{0,z} = \frac{2\pi}{\lambda} \sin\theta \tag{1}$$

Variation in the range of $k_{0,z}$ is achieved via rotation of the sample with respect to the incident beam, thereby varying θ.

The principles of neutron reflectivity have been extensively treated in the literature,[21,28] and the data analysis procedures have been discussed previously.[25] These will not be reproduced here. It should be noted, however, that the instrumental resolution in k_0 space is given by

$$\frac{\delta k_0}{k_0} = \frac{\delta\theta}{\theta} + \frac{\delta\lambda}{\lambda} \tag{2}$$

and because the incident collimation is fixed ($\delta\theta = 0.03°$), the reflectivity curves measured at different angles, θ, contain different resolution functions. Consequently, reflectivity profiles measured at different θ's cannot be superposed. Rather than desmearing the measured reflectivity profiles, the resolution function at each angle is convoluted with theoretically calculated reflectivity profiles and compared to the experimental profiles. The resolution function is assumed to be Gaussian with a full-width at half-maximum of δk_0.

3. Results and Discussion

The reflectivity profiles for the H/D:D/H, i.e., when both blocks of the copolymer are perdeuterated specimens as a function of k_0, are shown in Figure 1. The three different sets of data, displaced 1 decade from each other for clarity, represent measurements performed at incident angles 0.27°, 0.78°, and 1.46°. As mentioned earlier, the resolution function is different at each angle, and, as can be seen, features that are evident at high-angle measurements are smeared out in the low-angle measurements due to the poorer resolution. The solid lines are the calculated reflectivities using the scattering length density

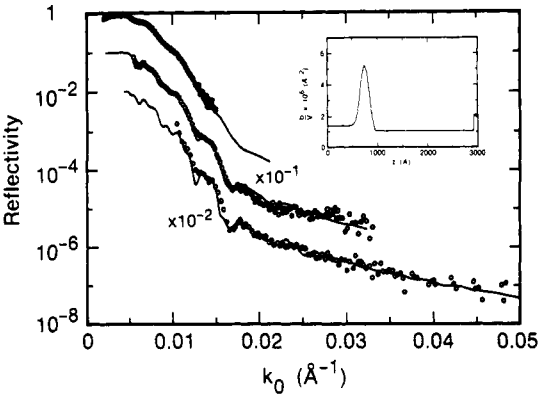

Figure 1. Experimental neutron reflectivity profile (O) for a trilayer on a silicon substrate. The trilayer is comprised of PS homopolymer at the air surface, a perdeuterated PS/PMMA diblock copolymer, and a PMMA layer adjacent to the substrate. Three different reflectivity results obtained at 0.27°, 0.78°, and 1.46° angles of incidence are shown. These have been offset for clarity by factors of 1, 0.1, and 0.01, respectively. The solid line represents the calculated reflectivity profile using the segment density profile shown in the inset.

profile shown in the inset. Use of a fully deuterated copolymer permits observation of the distribution of both copolymer blocks at the interface. The distribution of scattering length densities has a maximum of 5.2×10^{-6} Å^{-2}. The shape of the scattering length density profile was derived from halves of Gaussian distribution functions arising from the deuterated PS segments and deuterated PMMA segments in the copolymer. Due to the differences in the scattering length densities of the two components, differences in the molecular weights of the two blocks and slight differences in the statistical segment lengths of PS and PMMA, a single symmetric Gaussian would not be expected to suitably describe the results. The scattering length density profile begins at 1.4×10^{-6} Å^{-2} in the PS homopolymer phase, then rises to a maximum value of 5.2×10^{-6} Å^{-2}, and then falls off to a value of 1.06×10^{-6} Å^{-2} corresponding to that of the PMMA homopolymer. The standard deviations of the two Gaussian functions are 88 and 82 Å on the PS and PMMA sides of the interface, respectively. These correspond to widths of 150 and 140 Å, respectively.

The segment density profile of the PS segments in the diblock copolymer at the interface was isolated by deuterating only the PS segments of the block copolymer. This corresponds to an H/D:H/H trilayer specimen. Reflectivity profiles measured at angles of 0.27°, 0.78°, and 1.46° are shown in Figure 2. The solid lines are the calculated reflectivity profiles using the scattering length density profile shown in the inset. As with the perdeuterated diblock copolymer case, the scattering length density profile is a combination of halves of Gaussian functions beginning with a scattering length density of 1.43×10^{-6} Å^{-2} in the PS homopolymer phase, increasing to a maximum value of 4.0×10^{-6} Å^{-2}, and then falling off to a value of 1.06×10^{-6} Å^{-2} in the PMMA phase. The maximum value of the scattering length density profile is significantly less than that observed in the case of the perdeuterated diblock copolymer owing to the lower scattering length density of PS-*d* in comparison to that of PMMA-*d* and due to a penetration of some of the PMMA segments of the copolymer and homopolymer into the PS side of the interface. The standard deviations of the two Gaussian functions used were 74 and 29 Å on the PS and PMMA sides of the profile, respectively. These correspond to respective interfacial widths of 125 and 50 Å. The asymmetry of the distribution function is expected since

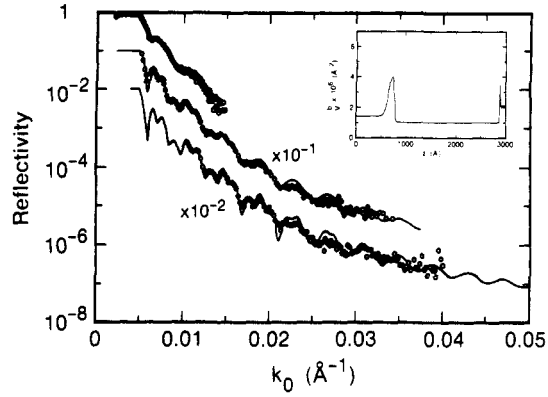

Figure 2. Same as in Figure 1, but now the trilayer is comprised of a PS layer at the air surface, a dPS/PMMA diblock copolymer at the homopolymer interface, and a PMMA layer adjacent to the substrate.

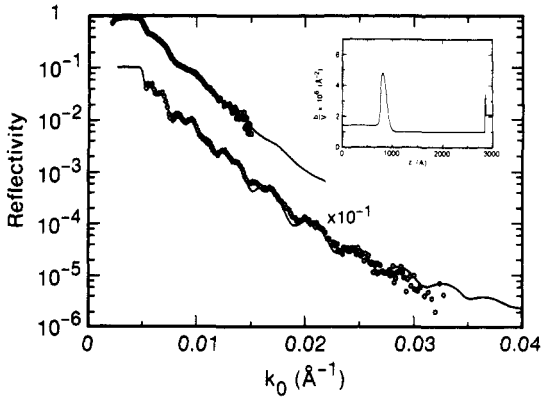

Figure 3. Experimental reflectivity profile (O) for a trilayer comprised of a PS layer, PS/PMMA-*d* copolymer at the homopolymer interface, and a PMMA layer adjacent to the substrate. The reflectivity profiles obtained at 0.3° and 0.8° angles of incidence have been offset by factors of 1.0 and 0.1, respectively, for clarity. The solid line is the calculated reflectivity profile using the scattering length density profile shown in the inset.

the penetration of the PS block into the PS phase will far exceed that of the PS into the interfacial region.

The segment density distribution of the PMMA segments of the copolymer at the interface was isolated by using a diblock copolymer where only the PMMA block was perdeuterated and the PS block, the PS homopolymer, and PMMA homopolymer were normal. This corresponds to a H/H:D/H trilayer specimen. The reflectivity profiles at 0.3° and 0.8° arising from this specimen are shown in Figure 3. Again the different profiles have been offset for clarity purposes only. As in the previous case, a scattering length density profile composed of halves of Gaussian functions was found to best describe the observed reflectivity data. This is shown in the inset of Figure 3. As expected, this segment density profile effectively mirrors that seen in the previous case, taking into account, of course, differences in the molecular weights and scattering length densities. The profile begins with the scattering length density of 1.43×10^{-6} Å^{-2} in the PS homopolymer phase, rises sharply to a value of 4.8×10^{-6} Å^{-2} at the maximum, and falls off more slowly to a value of 1.06×10^{-6} Å^{-2} in the PMMA phase. The maximum value of the scattering length density in this profile is only slightly less than that observed in the perdeuterated diblock copolymer case which can be associated with the penetration of the PS block of the copolymer and the PS homopolymer into the interfacial region. The standard deviations of the two Gaussian functions used were 29

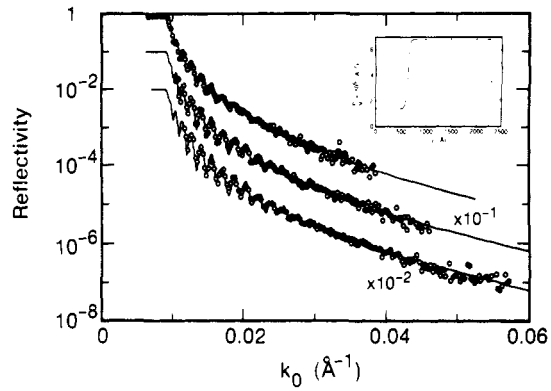

Figure 4. Same as in Figure 1, but now the trilayer is comprised of a layer of PS at the air surface, a PS/PMMA-*d* copolymer at the homopolymer interface, and a layer of PMMA-*d* adjacent to the substrate. The angles of incidence are 0.36°, 0.95°, and 1.48°.

and 74 Å on the PS and PMMA sides of the profile, respectively. These correspond to respective widths of 50 and 125 Å. These two values are essentially identical with that observed for the segment density profile of the PS segments of the block only mirrored across the interface.

The scattering length density profile in Figure 1 alone cannot reveal whether the copolymer blocks are segregated at the interface with the segments extending into their respective homopolymer phases or whether the copolymers and homopolymers are mixed with a preferential accumulation of the copolymer at the interface. However, Figures 2 and 3 unequivocally show that the copolymer blocks are indeed segregated at the interface, with the segments of each block penetrating significantly into the respective homopolymer phases. The fact that the scattering length density profiles of the PS and PMMA segments of the copolymer are sharp on the side closest to the interface suggests a uniform distribution of the junction points of the copolymers around the interface. The width of Gaussians on this side of the density profiles is comparable to the interfacial widths between the neat copolymer microdomains,[24,25] as well as, the interface width between the two homopolymers[23,25] with no added copolymer.

The measured reflectivity profile for the H/H:D/D trilayer is shown in Figure 4 corresponding to angles 0.36°, 0.95°, and 1.48°. This trilayer corresponds to the case where all the PMMA segments are perdeuterated and, therefore, is a measure of the interfacial behavior of the total PS and PMMA segments. The solid lines are the calculated reflectivities using the scattering length density profile shown in the inset. A smooth gradient in the scattering length density profile is found from 1.43×10^{-6} Å^{-2} for the pure PS to 6.8×10^{-6} Å^{-2} for the pure PMMA-*d*. The gradient can be best described by a hyperbolic tangent function with a width of 75 Å. This is much larger than the width of the interface formed between the PS and PMMA homopolymers and that formed between the microdomains of the pure diblock copolymer where an interfacial width of 50 Å was found.[25] Consequently, the presence of the diblock copolymer at the interface broadened the interfacial region by 50%, which is consistent with the large reduction of the interfacial tension.[6]

From the data presented thus far it should be possible to extract the segment density profiles of the blocks of the copolymers and the homopolymers at the interface by the solution of a simultaneous set of equations. It must be assumed that the differences in the molecular weights of the blocks of the different copolymer blocks are not significant. It should be mentioned, however, that the

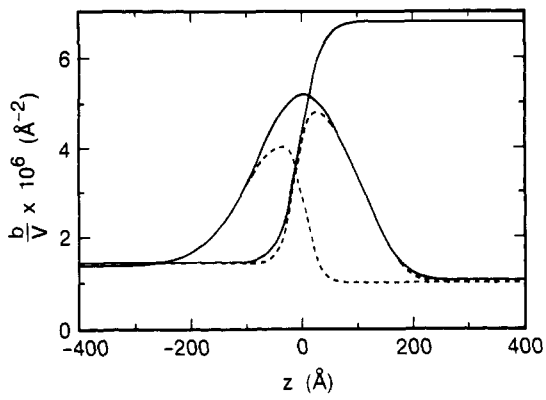

Figure 5. Composite diagram of the scattering length density profiles obtained from the reflectivity experiments shown in Figures 1–4. The different profiles correspond to the segment density profiles for the PS and PMMA block (- - -), the total copolymer (—), and the total PMMA segments (—), i.e., the summed PMMA segments. The profiles have been shifted horizontally to account for differences in the thickness of the upper homopolymer layers.

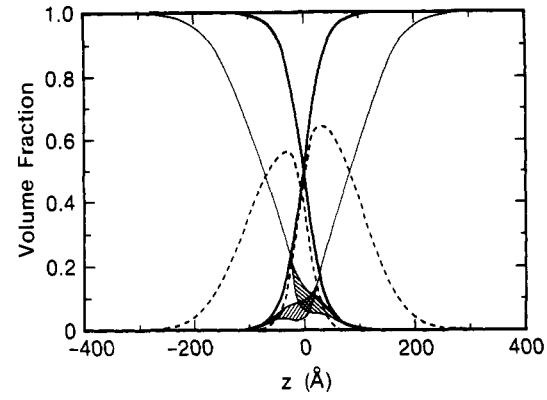

Figure 6. Volume fraction profiles of the PS and PMMA homopolymers (—), the PS and PMMA blocks of the copolymer (- - -), and the total PS and PMMA segments summed over the homopolymer segments and the respective blocks of the copolymer (—). These results were obtained by simultaneous solution of eqs 3 and 4, assuming that the molecular weights of the copolymers were identical. The cross-hatched regions represent uncertainties in the results for the homopolymer volume fraction profiles near the interface.

difference in the heights of the scattering length density profiles between the H/D:H/H and H/H:D/H specimens (Figures 2 and 3) cannot be explained completely by the difference in the scattering length densities of the individual components. Slight differences in the total amounts of the copolymer used and differences in the molecular weights may also contribute to this difference.

A composite diagram of the scattering length density profiles at the interface is shown in Figure 5. The scattering length densities in the insets of Figures 1–4 have been shifted horizontally in order to account for differences in the film thicknesses. Zero was placed at the peak of the H/D:D/H profile. The H/D:H/H and H/H:D/H profiles were shifted so that the distributions on the homopolymer sides of the profile overlapped. The H/H:D/D profile was adjusted in order to yield the best result in the analysis that follows.

The average scattering length density at a distance z from the surface is the weighted average of the scattering length densities of the homopolymer PS, the PS block of the copolymer, the PMMA block of the copolymer, and the homopolymer PMMA. The weighting is done according to the volume fractions, ϕ_i, of the components i. Therefore

$$b/V = \sum_i \phi_i (b/V)_i \tag{3}$$

and

$$\sum_i \phi_i = 1 \tag{4}$$

The scattering length density values for the individual components used are 1.43×10^{-6} Å^{-2} for normal PS, 6.1×10^{-6} Å^{-2} for deuterated PS, 1.06×10^{-6} Å^{-2} for normal PMMA, and 6.8×10^{-6} Å^{-2} for perdeuterated PMMA. Each of the four scattering length density profiles satisfies eq 3 and, with eq 4, forms a simultaneous set of linear equations. When the scattering length density profiles for the H/H:D/D, H/D:H/H, and H/H:D/H were used, the volume fractions of the individual components were derived from eqs 3 and 4, and these were used to calculate a scattering length density profile for the H/D:D/H system. This could, then, be compared with that determined experimentally.

Figure 6 shows the combined volume fractions of PS homopolymer, PS block, PMMA block, PMMA homopolymer, and the total PS and PMMA. The segregation of the individual blocks into their respective homopolymer domains is clearly evident. The characteristics of the individual profiles are shown in Table II. The differences in the peaks of the maximum values of the volume fractions of the PS and PMMA segments in the copolymer, as well as the differences in their full-width at half-maximum (fwhm), are, more than likely, due to the different block copolymers used, as discussed previously. The PS and PMMA homopolymers are found to be pushed apart at the interface with a "gap thickness" d_G, i.e., the distance between the midpoints of the PS and PMMA homopolymer profiles, of 154 Å or ca. 22.5 statistical segments (assuming an average statistical segment length of 6.85 Å[29]). However, it can be seen that homopolymers overlap significantly in the interfacial region. The effective width of the homopolymer profile, d_H, is 180 Å corresponding to 26 statistical segments, which is consistent with the large interpenetration. The total width of the interface between the PS and PMMA layers, d_T, is 75 Å, as mentioned earlier. It should be noted that the broadening of the interface to 75 Å in the presence of the copolymer mandates that the homopolymers penetrate deeply into the interface and overlap with each other in the interfacial region as is observed. The total concentration profile of the copolymer at the interface is shown as the heavy solid line in Figure 7 together with the profiles of the individual blocks. The maximum copolymer volume fraction is 0.85, whereas the maxima of the PS and PMMA blocks are 0.57 and 0.65, respectively. The fwhm is 180 Å, whereas the integrated copolymer concentration at the interface is

Table II
Volume Fractions

	ϕ_{max}[a]	fwhm,[b] Å	$\int_{-\infty}^{+\infty} \phi_i \, dz$,[c] Å
PS/PMMA copolymer	0.85	180	162
PS block	0.57	124	75
PMMA block	0.65	129	87

[a] Maximum volume fraction of the different constituents at the interface. [b] Full-width at half-maximum of the segment density profiles. [c] Integrated concentration at the interface.

$$\int_{-\infty}^{\infty} \phi_c \, dz = 162 \text{ Å} \tag{5}$$

where ϕ_c is the volume fraction of the copolymer. The scattering length density profile calculated for the H/D:D/H specimen using the volume fractions of the individual

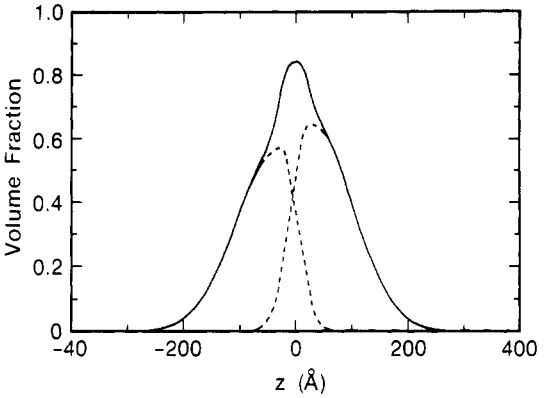

Figure 7. Volume fractions of the PS and PMMA segments of the copolymer (- - -) and the summed volume fraction of the total copolymer (—) obtained from eqs 2 and 3.

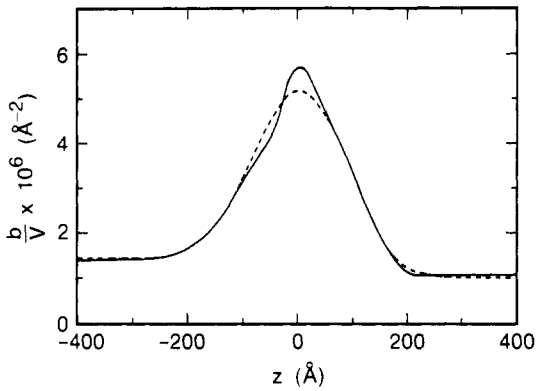

Figure 8. Comparison of the scattering length density profile for the H/D:D/H trilayer specimen to that calculated from the results in Figure 7.

species is compared to that derived from the reflectivity data in Figure 8. As can be seen, the agreement between the two is quite good showing the consistency of the experimental results. The maximum deviation from the experimental curve at the peak of the distribution is 10%. The slight asymmetry is due to the differences discussed earlier between segment density profiles of the PS and PMMA blocks. Taking this into account, the maximum volume fraction of the block copolymer at the interface is 0.81 ± 0.06.

From the copolymer distribution at the interface, one can calculate the area per copolymer chain at the interface. This is given by

$$\Sigma = \frac{\frac{M_1}{\rho_1} + \frac{M_2}{\rho_2}}{N_A \int_{-\infty}^{\infty} \phi_c \, dz} \tag{6}$$

where M_i is the molecular weight of block i with mass density ρ_i, N_A is Avogadro's number, and the integral is the integrated copolymer concentration. Assuming average values for the molecular weights of the blocks for the copolymers used in this study, i.e., 504 monomer units of PS and 543 monomer units of PMMA, or molecular weights 52 416 and 54 300, respectively, then Σ = 995.5 Å^2. With an average statistical segment length, a, of 6.85 Å, this yields

$$\Sigma = 21.2a^2 \tag{7}$$

With an average number of segments in the copolymer of 1100, our previous study[25] yields an average cross-sectional area per copolymer chain of 745 Å^2 in the bulk, lamellar microdomain morphology. Consequently, the copolymer chains at the homopolymer interface occupy 33% more area, which is in keeping with the result that the homopolymer chains penetrate deeply into the interfacial region.

Table III
Results of Reflectivity Measurements

sample designation	d_H,[a] Å	d_D,[a] Å	a_I,[b] Å
H/H:H/D	945	1615	229
H/H:D/D	775	1736	82
H/D:D/D	664	1903	182

[a] d_H and d_D are the thicknesses of the protonated and deuterated layers, respectively. [b] a_I is the effective width of the interface between the protonated and deuterated layers.

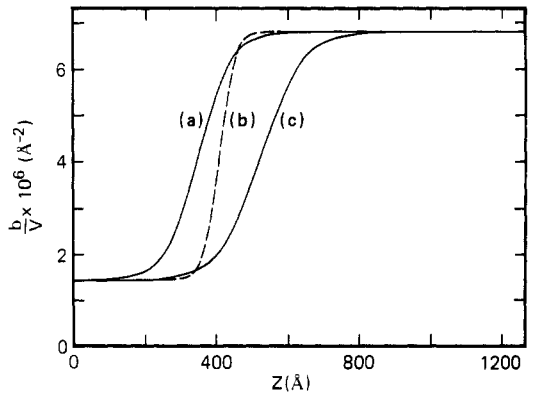

Figure 9. Composite scattering length density profile showing the scattering length densities obtained for the (a) H/D:D/D, (b) H/H:D/D, and (c) H/H:H/D experiments.

As a further test on the consistency of the scattering length density and segment density profiles determined from the reflectivity experiments, a second set of measurements was performed on a series comprised of H/H:H/D, H/H:D/D, and H/D:D/D trilayers. This series of experiments provided a unique means of reducing the number of parameters required to describe the reflectivity results. In each case, the scattering length density profiles can be described by a simple bilayer of protonated polymer on top of a layer of deuterated polymer. The roughness at the air/polymer interface is inconsequential due to the low scattering length density of the upper protonated layer. The thicknesses of each of the layers were determined independently by ellipsometry measurements. Consequently, the only adjustable parameter that is of importance is the interfacial width between the protonated and deuterated layers.

For brevity the reflectivity data are not shown in detail, but the results of the analysis are shown in Table III. The combined scattering length density profiles from these last three experiments are shown in Figure 9. The scattering length density profiles have been normalized on the distance scale so that the thicknesses of each layer are identical. It is now simply a matter of determining the differences between the three profiles to extract the segment density profiles of the individual components. For example, the difference between curve C (H/H:H/D) and curve B (H/H:D/D) yields the contribution to the scattering length density due to the methyl methacrylate segments of the copolymer. Similarly, the difference between curve B (H/H:D/D) and A (H/D:D/D) yields the contribution due to the styrene segments of the copolymer. Therefore, the volume fractions of all the components, be they from the homopolymers or copolymers, are directly obtained. It should be noted that this simple subtraction procedure leads to slightly negative values of the volume fractions of the components. While

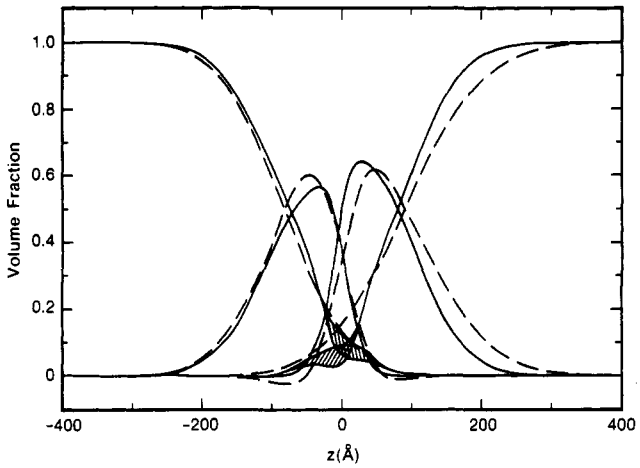

Figure 10. Comparison of the volume fractions of the PS and PMMA homopolymer segments and the PS and PMMA segments of the copolymers obtained from independent measurements on the H/D:H/H, H/H:D/D, and H/H:D/D series (—) and the H/H:H/D, H/H:D/D, and H/D:D/D series (– –) of specimens.

this is unrealistic, it does point to the errors in the determination of the scattering length density profiles and an insensitivity of the measurements to the exact functional form of the scattering length density profile. This, however, will not effect the conclusions that can be drawn.

A comparison of the volume fractions of the homopolymer and copolymer segments determined by the two different sets of experiments is shown in Figure 10. The solid lines represent the results from the H/D:H/H, H/H:D/H, and H/H:D/D series of experiments, whereas the dashed lines represent the results from the H/H:H/D, H/H:D/D, and H/D:D/D series of experiments. The results from these two independent studies are in excellent agreement with one another, well within any experimental uncertainties.

It is worthwhile to mention, at this point, that the evaluation of the different segment density distributions is very sensitive to the normalization of the distance scale in the profiles. While it was attempted to combine the neutron reflectivity results based on the thicknesses determined ellipsometrically, the reproducibility of the thicknesses of the lower PMMA layer and the thin copolymer layer from specimen to specimen was not better than ±20 Å. On an absolute and relative level, this error is not significant in comparison to this thickness of the individual layers. However, upon determination of the difference between the segment density profiles, these small errors will produce markedly different results. In fact, it is the error in the reproducibility of the sample thickness that places the major limits on the results shown in Figures 6 and 10. At present, a means of improving the reproducibility of the specimen thickness to within these limits is not known to us. The use of two different labeling schemes, however, significantly reduces the errors in the end results and substantially enhances the confidence in the derived volume fraction profiles.

For the copolymers and homopolymers used in this study (1221 monomer units for the PS homopolymer and 1211 monomer units for the PMMA homopolymer)

$$N_i < P_i^{3/2} \text{ and } \Sigma/a^2 < N_i^{1/2} \tag{8}$$

where N_i and P_i are the degrees of polymerization of the copolymer blocks and homopolymers of species i, respectively. According to the theory of Leibler,[14] such a system conforms to the "dry-brush" case where the copolymers are expected to be stretched and the homopolymers should not penetrate appreciably into the copolymer layer. In contrast to this, Figure 6 clearly shows a significant penetration of the homopolymers deep into the interface. For the dry-brush case, Leibler calculated the interfacial area per chain to be given by

$$\frac{\Sigma}{a^2} = \frac{3}{\sqrt{2}}\left(\frac{N}{\mu}\right)^{1/2} \tag{9}$$

where N is the total number of copolymer chains and μ is the equilibrium chemical potential of the copolymer in the interfacial "film", which is equal to that in the bulk. From eqs 7 and 9, this yields

$$\mu = 10.5 \tag{10}$$

The chemical potential μ is related to the copolymer volume fractions in the bulk phases by

$$\mu \simeq \ln \phi + 0.5\chi N \tag{11}$$

where χ is the Flory–Huggins interaction parameter, N is the total number of copolymer segments, and ϕ is the concentration of the copolymer in the bulk. Therefore, the "equilibrium" copolymer concentration in the bulk phases is of the order of $(0.6–3.0) \times 10^{-6}$, which is consistent with the reflectivity results. The lowering of the interfacial tension due to the presence of the copolymer chains is given by

$$\frac{\Delta\gamma a^2}{kT} = \frac{2^{3/2}}{9}\mu^{3/2}N^{-1/2} \tag{12}$$

or, $\Delta\gamma a^2/kT = 0.33$. The interfacial tension between the two homopolymers in the absence of a copolymer is predicted to be $\gamma_0 a^2/kT = 0.079$.

In a real situation, the interfacial tension decreases with the copolymer addition according to eq 12 up to some critical micelle concentration, cmc, when copolymer molecules in the bulk phases aggregate to form micelles. Assuming that the copolymers aggregate to form spherical micelles in the bulk, Leibler calculated the chemical potential of the copolymer at the cmc as

$$\mu_{cmc} = (3/2)^{4/3} f^{4/9}(\alpha f^{-1/3} - 1)^{1/3}(\chi N)^{1/3} \tag{13}$$

where $\alpha = 1 + 3\pi^2/40 = 1.74$ and f is the fraction of one kind of chains in the diblock copolymer. The copolymer concentration at the cmc is

$$\phi_{cmc} = \exp(\mu_{cmc} - f\chi N) \tag{14}$$

Also, the chemical potential, $\mu_{sat.}$, i.e., when the effective interfacial tension vanishes, is given by

$$\mu_{sat.} = (3/4^{2/3})(\chi N)^{1/3} \tag{15}$$

and the copolymer concentration is

$$\phi_{sat.} = \exp(\mu_{sat.} - f\chi N) \tag{16}$$

One should note that these relations hold for very high degrees of incompatibility ($\chi N > 54/f$) and for cases where the copolymers aggregate into spherical micelles. For the case here, $\chi N = 39 < 54/f$, the applicability of the equations to the polymers under study here may be questionable. Equations 13–16 yield $\mu_{cmc} = 4.5$, $\mu_{sat.} = 4.0$, $\phi_{cmc} = 6 \times 10^{-7}$, and $\phi_{sat.} = 4 \times 10^{-7}$. This means that, for spherical micelle formation, a vanishing interfacial tension will be achieved before the cmc. This vanishing interfacial tension will be achieved for copolymer concentrations less than in these experiments. This should lead to spontaneous curvature or "fingering" at the interfacial region. The instability at the originally flat interface would produce a broadening of the interfacial gradient as measured by

neutron reflectivity. However, the fact that all the experimental configurations discussed above resulted in very consistent scattering length density gradients does not indicate that such interfacial instabilities are present. The amount of copolymer present at the interface is still very high, and the system may be close to such an instability condition.

In addition, experiments have been recently performed[31] where the concentration or layer thickness of the copolymer has been varied. In all cases, the amount of off-specular scattering observed was low up to the point where the concentration of the copolymer corresponded to half the period of the copolymer in the bulk $L/2$. The interface was found to gradually broaden with increasing copolymer concentration. At concentrations in excess of the $L/2$ amount, the off-specular scattering markedly increased and the interface broadened significantly, indicating the formation of an interface with pronounced curvature or the formation of an ordered layer at the interface. Consequently, the results presented in this article represent an actual broadening of the interface between the styrene and methyl methacrylate monomers, i.e., a uniform change in the concentration of segments across the interface, and, since the off-specular scattering was low, cannot be attributed to a curvature of the interface.

4. Conclusion

Neutron reflectivity has been used to investigate the segment density distributions of diblock copolymers at the interface between two homopolymers. In the case of PS and PMMA homopolymers with the corresponding diblock copolymers, selective deuteration of either homopolymer or either block of the diblock copolymer has provided a means by which the individual components at the interface could be examined. It was found that the addition of the copolymer to the interface between the homopolymers significantly broadened the interface between the PS and PMMA homopolymers over that seen for the pure copolymer or that between the PS and PMMA homopolymers. It has been shown that the diblock copolymers are located at the interface between the homopolymers and that the PS segments of the copolymer were located in the PS phase and the PMMA segments of the copolymer in the PMMA phase. It was also found that the junction points of the copolymer were localized to a region around the midpoint of the interface over a distance comparable to the interfacial width observed for the neat diblock copolymers.

Furthermore, results from a series of experiments were used to solve a simultaneous set of linear equations that yielded the segment density profiles of the two homopolymers, of each block of the copolymer, and of the total copolymer at the interface. Results from this analysis were shown to be consistent with independent experimental results. This treatment showed that the homopolymers penetrated well into the interfacial region in contrast to theoretical arguments, which would place the copolymer in the dry-brush regime.

Acknowledgment. This work was supported by the Department of Energy, Office of Basic Energy Sciences, Grant No. FG03-88ER45375. Work at Argonne was performed under the auspices of the U.S. Department of Energy, Office of Basic Energy Sciences, under Contract W31-109-ENG-38.

References and Notes

(1) Molau, G. E. In *Block Copolymers*; Aggarwal, S. L., Ed.; Plenum Press: New York, 1970.
(2) Riess, G.; Periard, J.; Jolivet, Y. *Angew. Chem. Int. Ed. Engl.* **1972**, *11*, 339.
(3) Platzer, N. A. J., Ed. *Copolymers, Polyblends, and Composites*; Advances in Chemistry Series 142; American Chemical Society: Washington, DC, 1975; p 243.
(4) Fayt, R.; Jérôme, R.; Teyssié, Ph. *J. Polym. Sci., Polym. Lett.* **1986**, *24*, 25.
(5) Ouhadi, T.; Fayt, R.; Jérôme, R.; Teyssié, Ph. *Polym. Commun.* **1986**, *27*, 212.
(6) Anastasiadis, S. H.; Gancarz, I.; Koberstein, J. T. *Macromolecules* **1989**, *22*, 1449.
(7) Heikens, D.; Barentsen, W. M. *Polymer* **1977**, *18*, 70.
(8) Fayt, R.; Jérôme, R.; Teyssié, Ph. *J. Polym. Sci., Polym. Lett.* **1981**, *19*, 79.
(9) Brown, H. R. *Macromolecules* **1989**, *22*, 2859.
(10) Noolandi, J.; Hong, K. M. *Macromolecules* **1982**, *15*, 482.
(11) Noolandi, J. *Polym. Eng. Sci.* **1984**, *24*, 70.
(12) Noolandi, J.; Hong, K. M. *Macromolecules* **1984**, *17*, 1531.
(13) Leibler, L. *Macromolecules* **1982**, *15*, 1283.
(14) Leibler, L. *Makromol. Chem., Macromol. Symp.* **1988**, *16*, 1.
(15) Duke, T. A. J. Ph.D. Thesis, University of Cambridge, Cambridge, U.K., 1989.
(16) Hong, K. M.; Noolandi, J. *Macromolecules* **1981**, *14*, 72.
(17) Edwards, S. F. *Proc. Phys. Soc. London* **1965**, *85*, 613.
(18) de Gennes, P.-G.; Taupin, C. *J. Phys. Chem.* **1982**, *86*, 2294.
(19) de Gennes, P.-G. *Macromolecules* **1980**, *13*, 1069.
(20) Milner, S. T.; Witten, T. A.; Cates, M. E. *Macromolecules* **1988**, *21*, 2610.
(21) Werner, S. A.; Klein, A. G. In *Neutron Scattering*; Sköld, K., Price, D. L., Eds.; Academic Press: New York, 1986.
(22) Russell, T. P.; Karim, A.; Mansour, A.; Felcher, G. P. *Macromolecules* **1988**, *21*, 1890.
(23) Fernandez, M. L.; Higgins, J. S.; Penfold, J.; Ward, R. C.; Shackleton, C.; Walsh, D. J. *Polymer* **1988**, *29*, 1923.
(24) Anastasiadis, S. H.; Russell, T. P.; Satija, S. K.; Majkrzak, C. F. *Phys. Rev. Lett.* **1989**, *62*, 1852.
(25) Anastasiadis, S. H.; Russell, T. P.; Satija, S. K.; Majkrzak, C. F. *J. Chem. Phys.* **1990**, *92*, 5677.
(26) Russell, T. P.; Anastasiadis, S. H.; Satija, S. K.; Majkrzak, C. F., submitted for publication in *Phys. Rev. Lett.*
(27) Whitmore, M. D.; Noolandi, J. *Macromolecules* **1985**, *18*, 657.
(28) Felcher, G. P.; Hilleke, R. O.; Crawford, R. K.; Haumann, J.; Kleb, R.; Ostrowski, G. *Rev. Sci. Instrum.* **1987**, *58*, 609.
(29) Russell, T. P.; Hjelm, R. P.; Seeger, P. *Macromolecules* **1989**, *23*, 890.
(30) Russell, T. P. *Mater. Sci. Rep.* **1990**, *5*, 171.
(31) Russell, T. P.; Menelle, A.; Hamilton, W.; Smith, G.; Satija, S. K.; Majkrzak, C. F.; *Macromolecules*, submitted.

Registry No. P(S-*b*-MMA), 106911-77-7; PS, 9003-53-6; PMMA, 9011-14-7; neutron, 12586-31-1.